ARTICLE NO. 78-1295R

Approach Guidance Logic for a Tilt-Rotor Aircraft

Jacques Beser*
Intermetrics, Inc., Huntington Beach, Calif.

The distinctive feature of a tilt-rotor aircraft is that the pilot can change the rotor mast angles to go from a helicopter configuration for takeoff and landing to an airplane configuration for high cruise speeds, and vice-versa. An approach path for such an aircraft is proposed and the logic required to fly along this path in the presence of wind is determined. The main contribution of this work is an efficient and new method for generating the nominal state and control histories, taking into account an estimate of the mean wind velocity and direction. The method requires the solution of algebraic (mostly linear) equations to generate a "universal nominal," and feedforward and feedback gains. Then, in flight, the additional state and control corrections due to deviation in descent rate, deceleration, and flight in a steady wind are obtained by multiplying simple precalculated functions of time by the descent rate, deceleration, or sine and cosine components of the mean wind vector. Simulations of approach flights for different wind conditions, assuming perfect state information in the feedback signal, indicated satisfactory performance.

Nomenclature

a,R,h	= cylindrical components of aircraft mass center
D	= $1/K_G$ times integral of rpm error
L,M,N	= body-axes components of the aerodynamic/propulsive moments
p,q,r	= body-axes components of the aircraft angular velocity
Q_E,Q_R	= engine and rotor torques divided by rotor inertia
u,v,w	= body-axes components of the aircraft mass-center velocity
u_w,v_w,w_w	= body-axes components of the wind velocity
X,Y,Z	= body-axes components of the aerodynamic/propulsive forces divided by the aircraft mass
$\vec{x},\vec{T}$	= state and control vectors
Ω	= rotor rpm
Ω_0	= desired rotor rpm
ψ,θ,ϕ	= yaw, pitch, and roll Euler angles
θ_c	= rotor blade collective pitch

Introduction

AIRPORT congestion has suggested the use of short-haul aircraft whose approach and departure paths are in an airspace distinctly separate from the airspace used for CTOL approaches and departures. This led to the development of STOL, VTOL, and finally V/STOL technology, of which the tilt-rotor is an example.

The distinctive feature of a tilt-rotor aircraft is its ability to change its rotor mast angle to go from a hover configuration to a configuration for high cruise speeds, and vice-versa, making it well suited for intercity travel. This work uses the XV-15 tilt-rotor research aircraft as an example.

Presented as Paper 78-1295 at the AIAA Guidance and Control Conference, Palo Alto, Calif., Aug. 7-9, 1978; submitted Sept. 5, 1978; revision received April 10, 1979.

Index categories: Guidance and Control; Landing Dynamics; Simulation.

*Engineer. Member AIAA.

Path Definition

The selection of the approach flight path was based on the following considerations:

1) The available airspace for V/STOL approaches is often limited due to obstacles and/or CTOL traffic.
2) Flight in the helicopter configuration is noisy and requires a high rate of fuel consumption.
3) The XV-15 has limited deceleration capability in the airplane and transition modes; maximum deceleration for level flight at 160 knots in the airplane configuration is 0.15 g.
4) Approach should be possible from any direction.

To accommodate these requirements, we propose the following path:

1) The aircraft would descend and decelerate along a shallow, straight path while converting to its helicopter configuration.
2) When conversion is completed, it would descend on a spiral path while continuing its deceleration. The aircraft can fly more or less than one full turn along the spiral, depending on the particular requirements of the landing area. For example, a high spiral entry would provide good noise abatement.
3) Finally, it would fly a straight, descending, decelerating approach to a hover condition, then land. It is proposed to use a constant -6 deg flight-path angle for the spiral and straight final segments, and a -3 deg flight-path angle for the initial segment. The latter will allow deceleration even in the presence of a tailwind.

Given the position of the helipad, the descent cylinder location and radius, and the arrival direction, the nominal path is completely defined in space (see Fig. 1). However, the starting point on the initial segment (i.e., the "begin descent" point) will depend upon wind direction and magnitude. Flight-path angles for the different segments could be changed (keeping in mind the aircraft deceleration capability) to accommodate a particular landing site.

Manual tracking of such a complex path would appear to be quite difficult since the stability and control characteristics of the aircraft change rapidly with rotor-mast angle and airspeed. Therefore, this work develops logic for automatic generation and tracking of the path just described.

Aircraft Description[1,2]

The XV-15 tilt-rotor research aircraft is representative of those aircraft which will employ the tilt-rotor concept. The

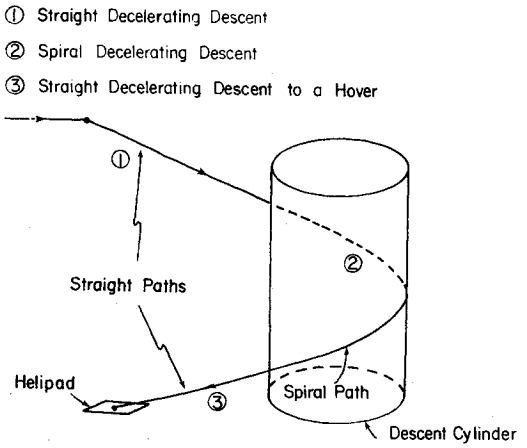

Fig. 1 Three-segment approach.

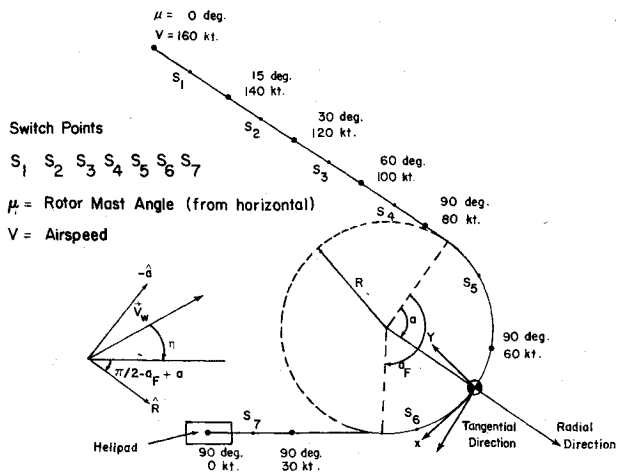

Fig. 2 Top view of normal path—model switching history.

hover lift and cruise propulsive force is provided by low disc loading rotors located at each wing tip. The rotor axes rotate from near vertical for helicopter flight to near horizontal for airplane flight. In the helicopter mode, control is provided by rotor-generated forces and moments while in the airplane flight mode, primary control is provided by conventional aerodynamic control surfaces.

Aircraft Controls

Cockpit controls will be used in the analysis and are described below. They are:

T_c = collective/power stick
T_L = longitudinal stick
T_l = lateral stick
T_p = pedals

Since the aircraft configuration can be changed from a helicopter to an airplane, both rotary-wing and fixed-wing controls are required. All are commanded through the four cockpit controls listed above. For a given mast angle, rotor controls and control surface motions due to cockpit control motions are in a fixed ratio.

Rotor Speed Governor

In the helicopter and transition modes, collective/power lever motion simultaneously changes the engine throttles and the rotor collective pitch. In the airplane mode, the collective/power lever controls only the engine throttles as the collective pitch input is phased out as a function of mast angle. In addition, power management is simplified by the automatic inputs of a governor which adjusts collective pitch to maintain the rotor rpm selected by the pilot.

Overall View of Guidance/Control Procedure

The original aircraft equations are of the form

$$\dot{\vec{x}} = f(\vec{x}, \vec{T}, t)$$

Table 1 Equilibrium points

Airspeed, knots	Mast angle, deg	Mode
160	0	airplane
140	15	transition
120	30	↓
100	60	↓
80	90	helicopter
60	90	↓
30	90	↓
0	90	↓

These equations are linearized about eight "equilibrium" points to yield equations of the form

$$\dot{\vec{x}} = F_i \vec{x}(t) + G_i \vec{T}(t)$$

where F_i and G_i are constant matrices for each equilibrium point. The superposition property of a linear system is used to calculate the nominal path commands, by adding the commands to fly a "universal" nominal to those required to fly the particular path considered.

Feedback control is performed using constant-gain matrices for each of the eight equilibrium points.

Nominal Path Commands – Spiral Segment

Description

The aircraft stability and control characteristics change significantly with mast angle and with velocity. Therefore, a single mathematical model cannot be used to represent the aircraft over the entire approach path. In view of this, the aerodynamic/propulsive forces and moments and the rotor torque were represented in terms of equilibrium values plus stability derivatives at several points along the approach path. This was done using a nonlinear simulation of the XV-15 and available reports.[1] The equilibrium points chosen correspond to wings-level straight descent at a −6 deg flight-path angle; the airspeeds range from 160 knots to 0 knots. The flaps were deflected 40 deg and the flaperons 25 deg for all cases. The equilibrium points chosen are listed in Table 1.

Switches from one equilibrium point to another were made when the airspeed was halfway between the airspeeds of the two equilibrium points. A switching history is presented in Fig. 2.

Rigid-Body Equations of Motion for a Rotary-Wing Aircraft

Coordinate Systems

Let us consider the descent cylinder discussed earlier. The aircraft center-of-mass position is determined by cylindrical coordinates (a, R, h), as shown in Fig. 2.

An aircraft body-axes system (x, y, z) with origin at the center of mass is defined as follows: 1) the x-axis along the centerline and forward, 2) the y-axis along the right wing, and 3) the z-axis perpendicular to the x- and y-axes and downward.

Rotor Equations

We include the rotor-speed/governor dynamics in the equations since a previous study shows that the governor mechanization introduces a significant coupling between the rotor speed and the vehicle longitudinal rigid-body motions.[3]

These equations can be written

$$\dot{\Omega} = Q_E + Q_R$$
$$\dot{D} = K_G(\Omega - \Omega_0) \tag{1}$$

Using Euler angles (ψ, θ, ϕ) to define the orientation of the body axes relative to the cylindrical axes, the complete set of aircraft equations of motion is (where s = sine, c = cosine):

Position

$$\begin{bmatrix} R\dot{a} \\ -\dot{R} \\ -\dot{h} \end{bmatrix} = \begin{bmatrix} c\psi c\theta & -s\psi c\phi + c\psi s\theta s\phi & s\psi s\phi + c\psi s\theta c\phi \\ s\psi c\theta & c\psi c\phi + s\psi s\theta s\phi & -c\psi s\phi + s\psi s\theta c\phi \\ -s\theta & c\theta s\phi & c\theta c\phi \end{bmatrix} \begin{bmatrix} u \\ v \\ w \end{bmatrix}$$

Angular Orientation

$$\begin{bmatrix} \dot{\phi} \\ \dot{\theta} \\ \dot{\psi} + \dot{a} \end{bmatrix} = \frac{1}{c\theta} \begin{bmatrix} c\theta & s\theta s\phi & s\theta c\phi \\ 0 & c\theta c\phi & -c\theta s\phi \\ 0 & s\phi & c\phi \end{bmatrix} \begin{bmatrix} p \\ q \\ r \end{bmatrix}$$

Force

$$\dot{u} + qw - rv = X - gs\theta$$
$$\dot{v} + ru - pw = Y + gc\theta s\phi$$
$$\dot{w} + pv - qu = Z + gc\theta c\phi$$

Moment

$$I_{xx}\dot{p} - I_{xx}(\dot{r} + pq) - (I_{yy} - I_{zz})qr = L$$
$$I_{yy}\dot{q} - I_{xz}(r^2 - p^2) - (I_{zz} - I_{xx})pr = M$$
$$I_{zz}\dot{r} - I_{xz}(\dot{p} - qr) - (I_{xx} - I_{yy})pq = N$$

Rotor

$$\dot{\Omega} = Q_E + Q_R = Q$$
$$\dot{D} = K_G(\Omega - \Omega_0) \tag{2}$$

Desired Outputs

We have seen that the aircraft equations of motion consist of 14 equations with 14 states and 4 controls. Four desired output histories will therefore be needed to determine the state and control histories. We have chosen these outputs to be: 1) the three cylindrical components of the center-of-mass position history—$a(t)$, $R(t)$, $h(t)$; and 2) the lateral specific force history $Y(t)$. [$Y(t) \equiv 0$ for a coordinated turn]. Note that $a(t)$ and $h(t)$ are determined by specifying $\ddot{a}(t)$ and $\gamma(t)$, i.e. deceleration and flight-path angle, and initial values of a, $\dot{a}$, and h.

In the case of the spiral segment, we shall specify that the deceleration $\ddot{a}$, the flight-path angle γ, and the radial position R are constant. In addition, in the case of a coordinated turn, we also have

$$Y = 0 \tag{3}$$

Superposition of Commands

In order to simplify the calculations, we use a "universal" nominal path and then add the commands required to fly the particular path considered. For a spiral segment, the commands are derived in four steps: 1) we calculate the commands for a steady, descending turn with no wind; 2) we calculate the additional commands due to deviations in the descent rate from Eq. (1); 3) we calculate the additional commands due to deceleration; 4) we calculate the additional commands due to steady wind. The addition of all the aforementioned commands gives the necessary commands to fly along the spiral path in a steady wind.

Commands for No-Wind Steady Turn with Nominal Descent Rate

Velocity of Mass Center

For a flight-path angle γ_t, we obtain

$$\begin{bmatrix} u \\ v \\ w \end{bmatrix} = V \begin{bmatrix} c\gamma_t c\psi c\theta + s\gamma_t s\theta \\ c\gamma_t [c\psi s\theta s\phi - s\psi c\phi] - s\gamma_t c\theta s\phi \\ c\gamma_t [c\psi s\theta c\phi + s\psi s\phi] - s\gamma_t c\theta c\phi \end{bmatrix} \tag{4}$$

Body-Axes Components of Angular Velocity

For a steady turn,

$$\dot{\phi} = \dot{\theta} = \dot{\psi} = 0 \tag{5}$$

and

$$\dot{a} \triangleq \omega = V\cos\gamma_t / R \tag{6}$$

From Eqs. (2) we obtain

$$p = -\omega s\theta \qquad q = \omega c\theta s\phi \qquad r = \omega c\theta c\phi \tag{7}$$

Dynamic Force Equilibrium

$$V\omega c\gamma_t s\psi c\theta = X - gs\theta$$
$$V\omega c\gamma_t (s\psi s\theta s\phi + c\psi c\phi) = Y + gc\theta s\phi$$
$$V\omega c\gamma_t (s\psi s\theta c\phi - c\psi s\phi) = Z + gc\theta c\phi \tag{8}$$

Expressions for Aerodynamic/Propulsive Forces

We have mentioned that the available data (equilibrium values and stability derivatives) were for a straight, constant-speed descent at a -6 deg flight-path angle. The aerodynamic/propulsive forces are expressed as these equilibrium (or trim) values plus additional terms for small perturbations from the straight descent:

$$\begin{aligned} X &= gs\theta_t + X_u\delta u + X_w\delta w + X_{\theta_c}\delta D + X_{T_c}\delta T_c + X_{T_L}\delta_{T_L} \\ Y &= Y_v v + Y_p p + Y_r r + Y_{T_l}\delta T_l + Y_{T_p}\delta T_p \\ Z &= -gc\theta_t + Z_u\delta u + Z_w\delta w + Z\theta_c\delta D + Z_{T_c}\delta T_c + Z_{T_L}\delta T_L \end{aligned} \tag{9}$$

Dynamic Moment Equilibrium

The angular momentum being constant for a steady turn, the aerodynamic/propulsive moments on the vehicle are zero.

Expressions for Aerodynamic/Propulsive Moments

As for the forces, we express the moments as the trim values plus additional terms for small perturbations from the straight descent. We obtain

$$\begin{aligned} L &= L_v v + L_p p + L_r r + L_{T_l}\delta T_l + L_{T_p}\delta T_p \\ M &= M_u\delta u + M_w\delta w + M_q q + M_{\theta_c}\delta D + M_{T_c}\delta T_c + M_{T_L}\delta T_L \\ N &= N_v v + N_p p + N_r r + N_{T_l}\delta T_l + N_{T_p}\delta T_p \end{aligned} \tag{10}$$

Rotor Equations

Nominally, the rotor rpm is constant

$$\Omega = \Omega_0 \tag{11}$$

The rotor torque, $Q_E + Q_R$, in Eq. (1) may be written as

$$Q_E + Q_R = Q_u\delta u + Q_w\delta w + Q_q\delta q + Q_{\theta_c}\delta D + \left(\frac{P_{T_c}}{I_R\Omega_0} + \frac{\partial\theta_c}{\partial T_c}Q_{\theta_c}\right)\delta T_c + Q_{T_L}\delta T_L \tag{12}$$

Coordinated Turn

For a coordinated turn, the lateral specific force is zero, i.e.,

$$0 = Y = Y_v v + Y_p p + Y_r r + Y_{T_l}\delta T_l + Y_{T_p}\delta T_p \tag{13}$$

Summary of Equations and Unknowns for a Steady, Descending Turn

1) For a steady, descending, coordinated turn, V, γ, and ω are specified. In addition, $Y=0$.

2) There are 17 equations: three each in Eqs. (4), (7), (8), (9), and (10), and one each in Eqs. (11) and (13).

3) There are 17 unknowns: (ψ, θ, ϕ), (p, q, r), (u, v, w), (D), (X, Y, Z), and (T_c, T_L, T_l, T_p).

Assuming small angles θ, ψ, and γ_t and eliminating some of the variables, we obtain Eqs. (14). Thus, specification of the speed V and spiral radius R determine $\omega \triangleq V/R$. Then we can solve for ϕ and δu.

Next, ϕ and δu gives us $\delta\theta$, δD, δT_c, δT_L, ψ, δT_l, and δT_p through Eqs. (14).

$$\begin{bmatrix} X_w V\mathrm{c}\phi - g & X_{\theta_c} & X_{T_c} & X_{T_L} & X_w V\mathrm{s}\phi - V\omega & 0 & 0 \\ Z_w V\mathrm{c}\phi & Z_{\theta_c} & Z_{T_c} & Z_{T_L} & Z_w V\mathrm{s}\phi & 0 & 0 \\ M_w V\mathrm{c}\phi & M_{\theta_c} & M_{T_c} & M_{T_L} & M_w V\mathrm{s}\phi & 0 & 0 \\ Q_w V\mathrm{c}\phi & Q_{\theta_c} & Q_{T_c} & Q_{T_L} & Q_w V\mathrm{s}\phi & 0 & 0 \\ \hline Y_v V\mathrm{s}\phi - Y_p\omega & 0 & 0 & 0 & -Y_v V\mathrm{c}\phi & Y_{T_l} & Y_{T_p} \\ L_v V\mathrm{s}\phi - L_p\omega & 0 & 0 & 0 & -L_v V\mathrm{c}\phi & L_{T_l} & L_{T_p} \\ N_v V\mathrm{s}\phi - N_p\omega & 0 & 0 & 0 & -N_v V\mathrm{c}\phi & N_{T_l} & N_{T_p} \end{bmatrix} \begin{bmatrix} \delta\theta \\ \delta_D \\ \delta_{T_c} \\ \delta_{T_L} \\ \hline \psi \\ \delta_{T_l} \\ \delta_{T_p} \end{bmatrix} = \begin{bmatrix} -X_u(V-u_t) - X_w V(\gamma_t-\theta_t)(1-\mathrm{c}\phi) \\ g(1-\mathrm{c}\phi) - Z_u(V-u_t) - Z_w V(\gamma_t-\theta_t)(1-\mathrm{c}\phi) - V\omega\mathrm{s}\phi \\ -M_q\omega\mathrm{s}\phi - M_u(V-u_t) - M_w V(\gamma_t-\theta_t)(1-\mathrm{c}\phi) \\ -Q_q\omega\mathrm{s}\phi - Q_u(V-u_t) - Q_w V(\gamma_t-\theta_t)(1-\mathrm{c}\phi) \\ \hline Y_v V(\gamma_t-\theta_t)\mathrm{s}\phi + Y_p\omega\theta_t - Y_r\omega\mathrm{c}\phi \\ L_v V(\gamma_t-\theta_t)\mathrm{s}\phi + L_p\omega\theta_t - L_r\omega\mathrm{c}\phi \\ N_v V(\gamma_t-\theta_t)\mathrm{s}\phi + N_p\omega\theta_t - N_r\omega\mathrm{c}\phi \end{bmatrix} \tag{14}$$

Perturbation from Steady Descending Turn

Let $\delta(\ )$ denote the deviation of $(\ )$ from its value in the steady descending turn. Taking the first variation of Eq. (2), noting that $\delta\Omega=0$, and adding the equation for $\delta Y=0$, we obtain 13 equations in 13 unknowns.

Additional Commands for Deviation in Descent Rate, $\delta\dot{h}_c$

For a steady descending turn, $\delta\dot{\phi}=\delta\dot{\theta}=\delta\dot{\psi}=0$. Also, $\delta\dot{a}=0$, $\delta R=0$, $\delta Y=0$ for a coordinated turn, and $u_w=v_w=w_w=0$.

For

$$\xi \triangleq [\delta\phi, \delta\theta, \delta\psi, \delta u, \delta v, \delta w, \delta p, \delta q, \delta r]^T$$

$$\lambda = [\delta T_c, \delta T_L, \delta T_l, \delta T_p]^T$$

Let

$$\xi = \delta\dot{h}_c \xi_\gamma \qquad \lambda = \delta\dot{h}_c \lambda_\gamma \tag{15}$$

The perturbation equations give

$$\left.\begin{array}{ll} 0 = F\xi_\gamma + G\lambda_\gamma & 9 \text{ eqs.} \\ b = C\xi_\gamma & 3 \text{ eqs.} \\ 0 = c\xi_\gamma + d\lambda_\gamma & 1 \text{ eq.} \end{array}\right\} \begin{array}{l} 13 \text{ eqs. in} \\ 13 \text{ unknowns} \end{array} \tag{16}$$

These equations can be solved for ξ_γ and λ_γ which are independent of $\delta\dot{h}_c$.

Additional Commands for Deceleration

Suppose that $R\delta\dot{a}=A_c t$, $\delta\dot{h}=0$, $\Delta R=0$; $\delta Y=0$ for a coordinated turn, and $u_w=v_w=w_w=0$.

Let

$$\xi = A_c(\xi_0 + \xi_1 t)$$

$$\lambda = A_c(\lambda_0 + \lambda_1 t)$$

and use

$$\delta\omega \simeq \delta V/R = (A_c/R)t \tag{17}$$

The perturbation equations give

$$\begin{aligned} \xi_1 &= F(\xi_0 + \xi_1 t) + G(\lambda_0 + \lambda_1 t) + (H/R)t \\ C(\xi_0 + \xi_1 t) &= bt \\ c(\xi_0 + \xi_1 t) + d(\lambda_0 + \lambda_1 t) &= 0 \end{aligned} \tag{18}$$

with

$$\xi \triangleq [\delta\phi, \delta\theta, \delta\psi, \delta u, \delta v, \delta w, \delta p, \delta q, \delta r]^T$$

and

$$\lambda \triangleq [\delta T_c, \delta T_L, \delta T_l, \delta T_p]^T$$

Identifying coefficients, we have

$$\left.\begin{array}{l} 0 = F\xi_1 + G\lambda_1 + H/R \\ C\xi_1 = b \\ c\xi_1 + d\lambda_1 = 0 \end{array}\right\} \begin{array}{l} 13 \text{ eqs. in} \\ 13 \text{ unknowns} \end{array} \tag{19}$$

$$\left.\begin{array}{l} \xi_1 = F\xi_0 + G\lambda_0 \\ C\xi_0 = 0 \\ c\xi_0 + d\lambda_0 = 0 \end{array}\right\} \begin{array}{l} 13 \text{ eqs. in} \\ 13 \text{ unknowns} \end{array} \tag{20}$$

We first solve Eqs. (19) for ξ_1 and λ_1, then use ξ_1 to solve Eqs. (20) for ξ_0 and λ_0.

Additional Commands Due to Steady Wind

In body axes, assuming all small θ and ψ, the wind can be written as (see Fig. 2)

$$\begin{bmatrix} u_w \\ v_w \\ w_w \end{bmatrix} = V_w \begin{bmatrix} c(a_F - a - \eta) + \psi\mathrm{s}(a_F - a - \eta) \\ (\theta\mathrm{s}\phi - \psi\mathrm{c}\phi)\mathrm{c}(a_F - a - \eta) + \mathrm{c}\phi\mathrm{s}(a_F - a - \eta) \\ (\theta\mathrm{c}\phi + \psi\mathrm{s}\phi)\mathrm{c}(a_F - a - \eta) - \mathrm{s}\phi\mathrm{s}(a_F - a - \eta) \end{bmatrix} \tag{21}$$

In the presence of wind, we still want the four output commands to be satisfied.

Let

$$\begin{aligned} \xi &= V_w[\xi_c \mathrm{c}(a_F - a - \eta) + \xi_s \mathrm{s}(a_F - a - \eta)] \\ \lambda &= V_w[\lambda_c \mathrm{c}(a_F - a - \eta) + \lambda_s \mathrm{s}(a_F - a - \eta)] \end{aligned} \tag{22}$$

Then

$$\dot{\xi} = V_w\omega\xi_c \mathrm{s}(a_F - a - \eta) - V_w\omega\xi_s \mathrm{c}(a_F - a - \eta) \tag{23}$$

Identifying coefficients, we obtain

$$\left.\begin{aligned} \omega\xi_c &= F\xi_s + G\lambda_s + K\eta_s \\ -\omega\xi_s &= F\xi_c + G\lambda_c + K\eta_c \\ C\xi_c &= 0 \\ C\xi_s &= 0 \\ c\xi_c + d\lambda_c &= 0 \\ c\xi_s + d\lambda_s &= 0 \end{aligned}\right\} \begin{array}{c} 26 \text{ equations} \\ \text{in} \\ 26 \text{ unknowns} \end{array}$$

Nominal Path Commands – Spiral Segment

In the previous sections, we have calculated the commands necessary for a steady descending turn and the additional commands for deviation in descent rate, deceleration, and steady wind. We can now add these different commands to obtain the required expressions for the nominal path. We obtain

$$\begin{aligned} \xi_N &= \xi_{ST} + \xi_\gamma \delta\dot{h}_c + (\xi_0 + \xi_1 t) A_c \\ &\quad + [\xi_c c(a_F - a - \eta) + \xi_s s(a_F - a - \eta)] V_w \\ \lambda_N &= \lambda_{ST} + \lambda_\gamma \delta\dot{h}_c + (\lambda_0 + \lambda_1 t) A_c \\ &\quad + [\lambda_c c(a_F - a - \eta) + \lambda_s s(a_F - a - \eta)] V_w \end{aligned} \tag{25}$$

where ST denotes the value corresponding to a steady descending turn with $\delta\dot{h}_c = A = V_w = 0$, i.e., a constant-velocity turn with no wind at the flight-path angle provided by the chosen equilibrium points.

It should be emphasized here that all feedforward gains due to deviation in descent rate, deceleration, or wind are independent of flight-path angle, deceleration, or wind velocity and direction. Therefore, they only have to be calculated once for each equilibrium point.

Nominal Path Commands – Straight Segments

The nominal path commands for the straight segments are derived using the same method as for the spiral segment.

Universal Nominal

The universal nominal is a straight descending flight at constant speed with no wind. This leads to four longitudinal equations and three lateral equations. These two sets are decoupled since

$$\psi_N = \phi_N = \omega_N = p_N = q_N = r_N = v_N = 0 \tag{26}$$

Perturbation Equations

Again, we use perturbation equations about the universal nominal path described above.

Crabbed Flight

In the case of a crabbed flight, we require zero sideslip, i.e.,

$$\delta v \equiv 0 \tag{27}$$

This is used in place of specifying zero lateral specific force as we did on the spiral segment.

Decrabbed Flight

When landing, it is preferable (although not required in the case of a landing from hover) to align the aircraft with its course. To do this, the aircraft must roll slightly into the crosswind. The amount of roll angle required is determined by specifying zero crab angle, i.e.,

$$\delta\psi = 0 \tag{28}$$

This is used in place of specifying zero lateral specific force as we did on the spiral segment.

The perturbation equations decouple into a longitudinal set and a lateral set as follows:

1) Longitudinal set: six equations with six unknowns (δu, δw, δq, $\delta\theta$, δT_c, δT_L).

2) Lateral set: six equations with six unknowns (δp, δr, $\delta\phi$, $\delta\psi$, δT_l, δT_p) for crabbed flight, (δv, δp, δr, $\delta\phi$, δT_l, δT_p) for decrabbed flight.

Additional Commands Due to Deviation in Descent Rate

This leads to the solution of six algebraic equations with six unknowns.

Initial Segment: Additional Commands for Constant Deceleration

This leads to the solution of two sets of six equations in six unknowns.

Final Segment: Additional Commands for Exponential Deceleration

After the aircraft leaves the spiral, it will start its final descent to a hover over the helipad. The use of a constant groundspeed deceleration along this segment would require a rather large step change to zero deceleration when hover is achieved, which would be uncomfortable. Therefore, we specify a groundspeed deceleration which is linearly decreasing with groundspeed, i.e., an exponentially decreasing deceleration with time. With this method, hover will be achieved at low final groundspeed deceleration and transition to zero deceleration will be smoother. Given the starting groundspeed, the distance to be traveled, and the initial deceleration, the exponential time constant required to end up at hover over the helipad is calculated.

Determination of the additional commands necessary for such a deceleration scheme leads to the solution of two sets of six equations with six unknowns.

Additional Commands Due to Steady Wind

This leads to the solution of four sets of six equations with six unknowns.

Nominal Path Commands – Straight Segments

As for the spiral segment, the commands necessary to fly the straight segments are obtained by adding the commands for the universal path to those obtained for deviations from this universal path. It is again emphasized that, except for the exponential deceleration, all feedforward gains have only to be calculated once for each equilibrium point and can therefore be stored in the aircraft computer. The feedforward gains due to exponential deceleration are simple functions of the exponential time constant and therefore present no difficulty.

Perturbation Feedback Control

Overall View of Guidance/Control Logic

The guidance/control logic used here is based on a rigid-body model of the aircraft and control signals of the form

$$T(t) = T_N(t) + C(t)[\hat{x}(t) - x_N(t)] \tag{29}$$

where

$$T \triangleq [T_c, T_L, T_l, T_p]^T$$

is the control vector, and

$$x \triangleq [p,q,r,u,v,w,\phi,\theta,\psi,x_0,R,h,\Omega,D,I_{x_0},I_R,I_h,u_g,v_g,w_g]^T$$

is the state vector;

$$\dot{I}_{x_0} = x_0 - x_{0_N} \qquad \dot{I}_R = R - R_N \qquad \dot{I}_h = h - h_N \tag{30}$$

are the integral error states; $[u_g, v_g, w_g]$ are wind gust states; C is the feedback gain matrix; $(\ )_N$ denotes nominal histories; and $\hat{x}$ denotes an estimate of the current state.

The gain matrix is piecewise constant, i.e., it is constant for each of the eight reference states used during the approach. We assume that $\hat{x}=x$, i.e., perfect knowledge of the state. In practice, some form of dynamic estimator would have to be used to find $\hat{x}$, which would lower the performance of the control system. Thus, the simulations indicate the best accuracy obtainable.

Gust Disturbance Model

In the presence of wind gust disturbances, gust feedback is helpful to control the aircraft. This section defines a gust disturbance model which will be used in determining the gust feedback gains.

We assume three components of wind gust velocity, u_g, v_g, and w_g. All three are modeled as stationary first-order zero-mean Gauss-Markov processes.[4] For the simulations in the next section, they are generated by passing white noise through a first-order shaping filter as follows:

$$\dot{u}_g = -\frac{1}{\tau_u} u_g + \epsilon_u \qquad \dot{v}_g = -\frac{1}{\tau_v} v_g + \epsilon_v \qquad \dot{w}_g = -\frac{1}{\tau_w} w_g + \epsilon_w \tag{31}$$

where ϵ_u, ϵ_v, and ϵ_w are independent white-noise processes with zero-mean and power spectral densities Q_u, Q_v, Q_w, respectively. If the rms values of u_g, v_g, w_g are respectively σ_{u_g}, σ_{v_g}, σ_{w_g}, we have the relations

$$Q_u = \frac{2\sigma_{u_g}^2}{\tau_u} \qquad Q_v = \frac{2\sigma_{v_g}^2}{\tau_v} \qquad Q_w = \frac{2\sigma_{w_g}^2}{\tau_w} \tag{32}$$

We used $\tau_u = \tau_v = 3$ s and $\tau_w = 2$ s and chose the power spectral densities so that σ_{ug}, σ_{vg}, and σ_{wg} were respectively 10, 10, and 6 ft/s.

Perturbation Equations of Motion

Taking the first variation of the nonlinear equations of motion (2) and including the gust equations (31) with the white noise equal to zero, we obtain perturbation equations of motion of the form

$$\delta\dot{x} = F(t)\delta x + G(t)\delta T \tag{33}$$

where

$$\delta x \triangleq x - x_N \qquad \delta T \triangleq T - T_N$$

The matrices F and G are piecewise constant, i.e., constant for each of the eight reference states used during the approach. For small bank angles, $|\phi| \ll 1$, the 20 equations of Eq. (33) nearly decouple into twelve longitudinal equations with two controls and eight lateral equations with two controls. Since the nominal bank angle is approximately 20 deg, we have used this decoupling assumption. The two systems are

Longitudinal

$$\delta x^{(L)} \triangleq [\delta u, \delta w, \delta q, \delta\theta, \delta\Omega, \delta D, \delta x_0, \delta h, I_{x_0}, I_h, u_g, w_g]^T$$

$$\delta T^{(L)} = [\delta T_c, \delta T_L]^T$$

Lateral

$$\delta x^{(l)} \triangleq [\delta v, \delta p, \delta r, \delta\phi, \delta\psi, \delta R, I_R, v_g]^T$$

$$\delta T^{(l)} = [\delta T_l, \delta T_p]^T$$

Quadratic Synthesis[4,5]

We use quadratic synthesis to determine the feedback gain matrices. If x is the state vector, and u the control vector, we form a performance index

$$J = \frac{1}{2}\int_0^\infty (x^T A x + u^T B u)\,dt$$

where A and B are weighting matrices, and $u = Cx$.

The problem consists of finding the gains C so as to minimize the performance index J. A and B matrices must be chosen carefully so as to limit the state excursions and the amount of control use. A good rule of thumb in determining the diagonal matrices A and B is to use for each state the inverse square of the maximum deviation one will allow this state, and for each control, the inverse square of the amount of control effort one is willing to commit to correct the state deviation.

This was done for each of the eight reference states. The resulting roots were not always well damped, and modifications to the initial weights selection were required in most cases.

Simulation of Controlled Flights

Overview

Digital simulations of five controlled flights were made with the wind disturbances shown in Table 2. The simulations were made using the equations of rigid-body motion as given by Eqs. (2). The gusts were generated by first-order shaping filters with white-noise inputs. Sampling intervals varied from 0.2 to 0.3 s, where the reciprocal of the real part of the fastest closed-loop eigenvalue was 0.3 s, and the shortest closed-loop period was 2.1 s.

Results plotted were control histories, position error histories, and nominal airspeed histories. The results of the first simulation are presented in this paper. Results of the other simulations are only discussed briefly.[6]

Switching Between Equilibrium Models

The simplest implementation of the guidance/control system proposed here, and of the digital simulation, uses instantaneous switching from one equilibrium model to the next when the airspeed is halfway between the two airspeeds of the equilibrium models. This introduces discontinuities in the stability derivatives, the feedforward gains, and the feedback gains which produce discontinuities in the control; these control discontinuities attenuate rapidly and look like "spikes" on our plotted results from the simulations. These spikes could be eliminated by linearly interpolating the stability derivatives and feedforward/feedback gains between each two equilibrium points. For computer economy, we did not do this in our simulations.

Table 2 Digital simulations of controlled flights

Case	Mean wind	Gusts
1	Estimate correct	None
2	Estimate incorrect	None
3	Estimate correct	Severe gust, with gust feedback
4	Estimate correct	Severe gust, without gust feedback
5	Wind shear; estimate correct	None

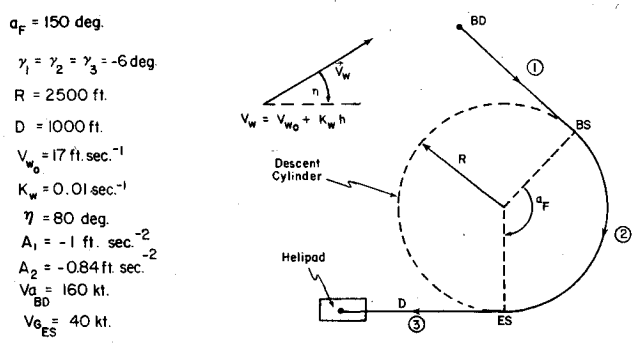

Fig. 3 Nominal flight path, cases 1, 2, 3, and 4.

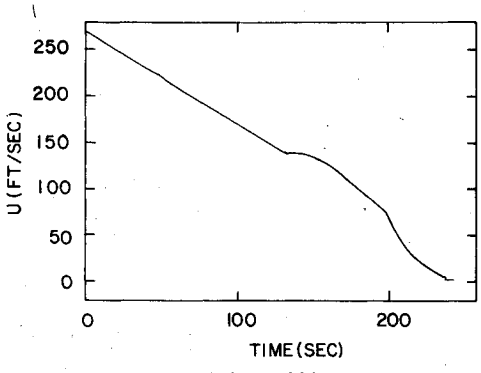

Fig. 4 Forward airspeed history, case 1.

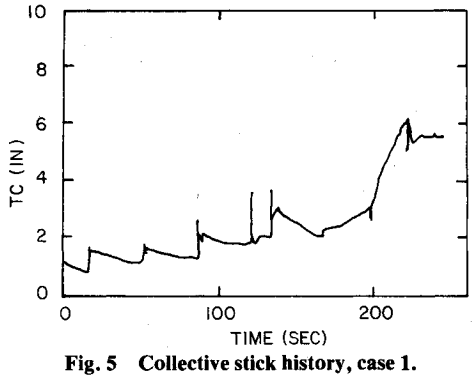

Fig. 5 Collective stick history, case 1.

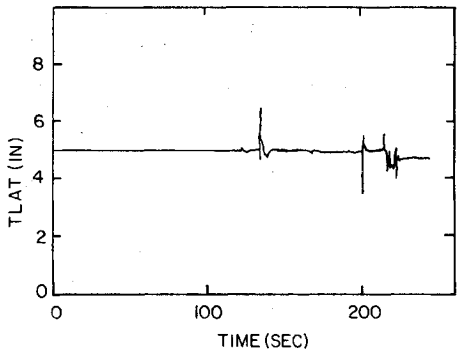

Fig. 6 Lateral stick history, case 1.

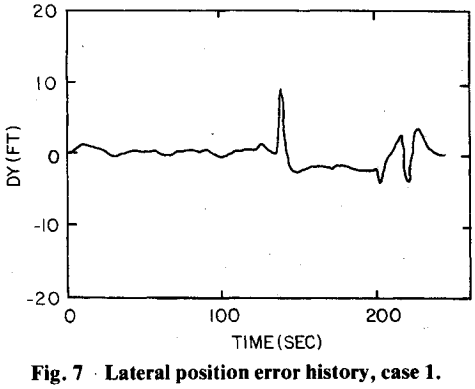

Fig. 7 Lateral position error history, case 1.

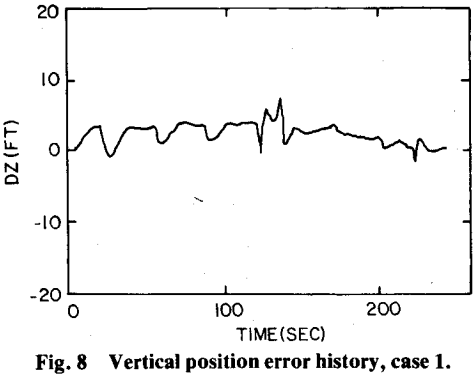

Fig. 8 Vertical position error history, case 1.

The first few switches also involve an instantaneous change in rotor mast angles. In practice, it takes about 2 s to change the mast angles through 15 deg. Again, for computer economy, we used instantaneous switches.

Simulation 1: Mean Wind Estimate Correct, No Gusts

The nominal path is defined in Fig. 3. For simulation 1, the mean wind profile is known exactly.

In Fig. 4, the constant airspeed deceleration is apparent on segment 1 during conversion from the airplane to the helicopter configuration. At the spiral entry, a slight increase in airspeed occurs because the aircraft is turning into the wind. In the third segment, airspeed decreases exponentially due to an exponentially decreasing groundspeed deceleration command. Finally, the airspeed stabilizes at a nonzero value at hover in the given mean wind.

In Fig. 5, there are discontinuities in collective stick setting when switching from one model to another. The spikes were explained except for the large spike occuring at spiral entry, which produces the extra power required when the aircraft is banked. Correspondingly, a smaller spike occurs at spiral exit, due to power decrease. After the switch to the 60-knots model, the collective increases as the aircraft wing is approaching stall conditions.

In Fig. 6, deviations at about 215 s are due to the decrab maneuver and the switch to the hover model.

The lateral position error (Fig. 7) shows $R - R_N$ to be very small except for a 10-ft error while entering the spiral. Some minor lateral motions also take place at spiral exit and during the decrab maneuver. Final lateral error is negligible.

In Fig. 8, the altitude is a little high for most of the flight, with a maximum error of 10 ft. However, final altitude error is negligible.

In summary, tracking in the case of a known wind profile was quite successful. Forward position errors were less than 23 ft. for a total flight of over 30,000 ft, and lateral and vertical position errors were less than 10 ft. Moreover, the final position was accurate to within 1 ft in all three dimensions, and control activity was reasonable throughout.

Simulation 2: Mean Wind Estimate Incorrect, No Gusts

In this case, we use a different mean wind profile in the open-loop calculations and in the simulation. The nominal mean wind information is the same as used in the previous case. For the simulation, we assume a 5-deg error in direction to 75 deg, a wind profile slope of 0.006 (ft/s)/ft and a 25 ft/s wind velocity at ground level. Temporary errors in position

occur while the integral error states build up. Maximum forward error is a loss of 60 ft with a final error of about 3 ft. Lateral position error reaches a peak of 18 ft initially and while flying the spiral segment. Final lateral error is negligible. Altitude error reaches a peak of 9 ft at spiral entry, with a negligible final error.

Simulations 3 and 4: Mean Wind Estimate Correct, Gusts with/without Gust Feedback

The mean wind profile is the same as used in the previous simulations.

We assume gusts in all three directions (x,y,z), as described earlier. The gust generation equations with $\epsilon_u = \epsilon_v = \epsilon_w = 0$ were included in the feedback gain synthesis so that feedback gains on u_g, v_g, and w_g were produced. Use of gust feedback reduces control activity and improves tracking. Of course, we must keep in mind the assumption made for "perfect knowledge of the states" which, in the case of gusts in particular, is not realistic.

There is considerable control saturation. Therefore, it would be wise to reset the gains to lower values and "ride" the gusts by allowing larger deviations from the path. Of course, when approaching the landing site, tight control is required, but, at low altitude, gusts are generally not as intense as represented here.

Simulation 5: Wind Shear, Estimate Correct, No Gusts

In this case we consider a strong wind shear on the last 1000 ft of the descent (5 ft/s per 100 ft). The simulation was started in the helicopter mode at 80 knots. The position errors were quite small throughout the flight, with maximum forward position error of the order of 10 ft and 2 ft at hover, maximum lateral position error of the order of 5 ft and negligible terminal error, and altitude error quite small throughout the flight, with a maximum of 7 ft reached at the start of the final approach (due to a large deceleration change) and negligible terminal error.

Conclusions

Guidance logic for performing a decelerating spiral approach of a tilt-rotor aircraft in the presence of wind has been developed. The logic consists of nominal (feedforward) commands plus feedback commands to the four cockpit controls. All feedback and feedforward gains are precalculated (except for the feedforward gains associated with the exponential deceleration, which are simple functions of the exponential time constant). A rigid-body model was used since, at low speeds, the motion of the mass center is strongly coupled to the angular motions of the aircraft, and vice versa. Perfect state information was assumed in the simulations. The degradation in performance due to the use of estimators and various sensors should be investigated, as well as an improved logic for a smooth switching from one mathematical model to the next. A weighting technique is suggested. Longitudinal-lateral coupling in the spiral turn was neglected in computing the feedback gains. Inclusion of this coupling will lead to many more gains and it is not clear whether the improvement in accuracy is significant enough to warrant this complication.

Acknowledgments

The author wishes to acknowledge the advice and guidance of A.E. Bryson and the stimulating discussions with H. Erzberger. This research was performed under NASA Grant 05-020-007 from the NASA Ames Research Center.

References

[1] Anon., "V/STOL Tilt-Rotor Research Aircraft," Vols. 1-4, Bell Helicopter Company, Reports No. 301-199-001,002,003, and 301-099-001, Jan. 1973.

[2] Maisel, M., "Tilt-Rotor Research Aircraft Familiarization Document," NASA Ames Research Center and U.S. Army Air Mobility R&D Laboratory, Moffett Field, Calif., NASA TMX-62, 407.

[3] Radford, R.C., Schelhorn, A.E., Siracuse, R.J., et al., "Evaluation of XV-15 Tilt-Rotor Aircraft for Flying Qualities Research Application," CALSPAN Corporation, Buffalo, N.Y., Tech. Report. AK-5752-F-1, April 1976, NASA CR-137828.

[4] Bryson, A.E. Jr. and Ho, Y.C., *Applied Optimal Control,* Blaisdell Publishing Co., Waltham Mass., 1969.

[5] Bryson, A.E. Jr. and Hall, E.W., "Optimal Control and Filter Synthesis by Eigenvector Decomposition," Department of Aeronautics and Astronautics, Stanford University, Stanford, Calif., SUDAAR 436, Dec. 1971.

[6] Beser, J., "Guidance Logic for Decelerating Spiral Approach of a Tilt-Rotor Aircraft in the Presence of Wind," Department of Aeronautics and Astronautics, Stanford University, Stanford, Calif., SUDAAR 506, Dec. 1977.